The International Journal of Biochemistry & Cell Biology 53 (2014) 186–194

Contents lists available at ScienceDirect

The International Journal of Biochemistry & Cell Biology

journal homepage: www.elsevier.com/locate/biocel

Increased expression of prostaglandin reductase 1 in hepatocellular carcinomas from clinical cases and experimental tumors in rats

Ricardo Sánchez-Rodríguez[a], Julia Esperanza Torres-Mena[a,b], Monica De-la-Luz-Cruz[a], Gloria Alejandra Bernal-Ramos[a], Saúl Villa-Treviño[b], Victoria Chagoya-Hazas[c], Luis Landero-López[d], Rebeca García-Román[e], Patrick Rouimi[f], Luis Del-Pozo-Yauner[a], Jorge Meléndez-Zajgla[a], Julio Isael Pérez-Carreón[a,*]

[a] Instituto Nacional de Medicina Genómica, México D.F., Mexico
[b] Departamento de Biología Celular, Centro de Investigación y de Estudios Avanzados del IPN, México D.F., Mexico
[c] Instituto de Fisiología Celular. Universidad Nacional Autónoma de México, México D.F., Mexico
[d] Centro de Especialidades Médicas del Estado de Veracruz "Dr. Rafael Lucio", Xalapa Veracruz, México D.F., Mexico
[e] Instituto de Salud Pública de la Universidad Veracruzana. Veracruz, Mexico
[f] Institut National de la Recherche Agronomique (INRA), UMR 1331 TOXALIM (Research Centre in Food Toxicology), Toulouse, France

ARTICLE INFO

Article history:
Received 10 February 2014
Received in revised form 3 May 2014
Accepted 7 May 2014
Available online 20 May 2014

Keywords:
Diethylnitrosamine
Alkenal/one oxidoreductase
Carcinogen detoxification enzymes
4-Hidroxynonenal
Tumor marker

ABSTRACT

To identify novel tumor-associated proteins, we analyzed the protein expression patterns from experimental hepatocellular carcinoma (HCC) that were induced using hepatocarcinogenesis models in rats. Rats were subjected to two previously described protocols of hepatocarcinogenesis using diethylnitrosamine as a carcinogen: the alternative Solt–Farber (aS&F) protocol, which induces HCC within 9 months, and Schiffer's model, which induces cirrhosis and multifocal HCC within 18 weeks. The patterns of protein expression from tumors and normal liver tissue were examined by SDS-PAGE and the bands identified at 33–34 kDa were analyzed by mass spectrometry. The prostaglandin reductase 1 (PTGR1) showed the highest number of peptides, with a confidence of level >99%. The increased expression of PTGR1 in tumors was confirmed in these two models by Western blotting and by increase in alkenal/one oxidoreductase activity (25-fold higher than normal liver). In addition, the gene expression level of *Ptgr1*, as measured by qRT-PCR, was increased during cancer development in a time-dependent manner (200-fold higher than normal liver). Furthermore, PTGR1 was detected in the cytoplasm of neoplastic cells in rat tumors and in 12 human HCC cases by immunohistochemistry. These analyses were performed by comparing the expression of PTGR1 to that of two well-known markers of hepatocarcinoma, Glutathione *S*-transferase pi 1 (GSTP1) in rats and glypican-3 in humans. The increased expression and activity of PTGR1 in liver carcinogenesis encourage further research aimed at understanding the metabolic role of PTGR1 in HCC and its potential application for human cancer diagnosis and treatment.

1. Introduction

Hepatocellular carcinoma (HCC) is the most common tumor of the liver and the third most common cause of cancer death worldwide. The limited treatment options for intermediate- and advanced-staged cancers (El-Serag et al., 2008) necessitate the search for additional biomarkers to detect liver cancer at early stages. Animal models of hepatocarcinogenesis are commonly used to study the multistep process of human liver carcinogenesis, particularly the preneoplastic stage (Libbrecht et al., 2005; Wu et al., 2009). There are two chemical hepatocarcinogenesis models in the rat that are induced with the carcinogen diethylnitrosamine (DEN) and produce HCC in different contexts of cirrhosis. The Solt and

Abbreviations: HCC, hepatocellular carcinoma; DEN, diethylnitrosamine; S&F, Solt and Farber model; LTB4, leukotriene B4; PGE2, prostaglandin E2; 15d-PGJ2, 15-deoxy-delta-12,14-prostaglandin J2; LXA4, lipoxin A4; 4HNE, 4-hydroxy-2-nonenal; GSTP1, glutathione *S*-transferase pi 1; GGT, γ-glutamyl transferase; PH, 70% partial hepatectomy; ENT, enriched nodular tissue; MS/MS, tandem mass spectra; TFA, trifluoroacetic acid; H&E, hematoxylin-eosin; ANOVA, analysis of variance; rRNA, ribosomal RNA; qRT–PCR, quantitative reverse transcriptase polymerase chain reaction; 2AAF, 2-acetylaminofluorene; mRNA, messenger RNA; cDNA, complementary DNA; NQO1, NAD(P)H dehydrogenase, quinone 1; GSTs, glutathione *S*-transferases; EPHX, epoxide hydrolase; GCL, glutamate-cysteine ligase; UGTs, UDP glucuronosyltransferases.

* Corresponding author. Tel.: +52 55 5350 1900x1170; fax: +52 55 5350 1999.
E-mail address: jiperez@inmegen.gob.mx (J.I. Pérez-Carreón).

http://dx.doi.org/10.1016/j.biocel.2014.05.017
1357-2725/

Farber (S&F) model induces nodules of resistant hepatocytes that resemble dysplasia, which chronologically progress into HCC without liver cirrhosis within a period of 9 months (Farber and Sarma, 1987; Solt and Farber, 1976). In contrast, Schiffer's model induces cirrhosis and multifocal HCC within 18 weeks (Schiffer et al., 2005).

In this work, we utilized proteomic technology to identify proteins expressed in experimental tumors. Among the proteins identified by mass spectrometry at 33–34 kDa, the top-ranked protein in the tumor samples was PTGR1. This enzyme possesses dual activity, as it is involved in the inactivation of eicosanoids with high biological activity such as leukotriene B4 (LTB4), prostaglandin E2 (PGE2), 15-deoxy-delta-12,14-prostaglandin J2 (15d-PGJ2), and lipoxin A4 (LXA4) (Clish et al., 2000; Hori et al., 2004; Yu et al., 2006), and it also has an antioxidative function through the NADPH-dependent reduction of the carbon–carbon double bond of a variety of unsaturated aldehydes and ketones such as 4-hydroxy-2-nonenal (4HNE), a cytotoxic lipid peroxidation product (Dick and Kensler, 2004). Additionally, PTGR1 reduces fatty acid nitroalkenes to nitroalkanes, inactivating the downstream signaling action of these reactive lipid electrophiles (Vitturi et al., 2013).

PTGR1 has been described as a cytoprotective enzyme that is induced in the rat liver following treatment with cancer chemopreventive agents such as dithiolethiones (Primiano et al., 1998). In this study, we measured PTGR1 expression at both the mRNA and protein levels over the course of liver cancer progression in two models of hepatocarcinogenesis in rats. In addition, PTGR1 was also studied in human HCC cases by immunohistochemistry. The expression of PTGR1 was evaluated as a potential biomarker by comparing its expression level to those of two well-known liver cancer markers, Glutathione *S*-transferase pi 1 (GSTP1) in rat tumors and glypican-3 in human tumors.

2. Material and methods

2.1. Animal procedures

Forty male F344 rats weighing 200 g were used for the two models of hepatocarcinogenesis: the alternative Solt and Farber (aS&F) protocol (Carrasco-Legleu et al., 2004; Marche-Cova et al., 1995) and the DEN-induced hepatocarcinogenesis model described by Schiffer et al. (2005) (Schiffer's protocol). Animals were obtained from the Animal Production and Experimentation Unit (UPEAL-Cinvestav, Mexico, DF, Mexico). All experiments followed committee guidelines and the institutional protocols for animal care. Groups of 20 rats for each protocol were treated as indicated in Fig. 1. Normal livers from a group of five adult rats (weighing 200–300 g) were used as controls. Animals were sacrificed by exsanguination under ether anesthesia, and then the livers were excised, washed in physiological saline solution, and frozen in 2-methylbutane with liquid nitrogen and stored at −70 °C. Nodular lesions were identified in histological sections according to gamma-glutamyltransferase (GGT) activity and then dissected from the frozen liver with a stainless steel cork borer (internal diameter, 1 mm) (Perez-Carreon et al., 2006). As a result, a collection of 20 nodules per liver was designated as enriched nodular tissue (ENT).

2.2. Protein extraction and mass spectrometry

The tissue samples (50 mg) were homogenized in 1 ml of lysis buffer containing 50 mM Tris–HCl, 150 mM NaCl, 0.25% Na-deoxycholate, 1 mM EDTA, and 1× of protease inhibitor cocktail (ProteoBlock, Fermentas). Equivalent amounts of protein (30 μg) were separated by 10% SDS-PAGE. Gels were stained with colloidal Coomassie blue. Unique bands were excised from the gels and processed for protein identification at INMEGEN's proteomics facility as described (Perez et al., 2010). Identification of the proteins from the peptides was performed using a 4800 Plus MALDI-TOF/TOF mass spectrometer (Applied Biosystems, USA). Tandem mass spectra (MS/MS) were analyzed using the Protein pilot software (Applied Biosystems), and the peak list of tandem mass spectra was submitted for a search against rat species in the UniProtKB/Swiss-Prot database using the Paragon algorithm.

2.3. Western blot analysis

Proteins (30 μg) were separated by 10% SDS-PAGE and transferred onto PVDF membranes (Millipore) by electroblotting. Membranes were blocked with 5% non-fat milk and then incubated overnight at 4 °C with mouse polyclonal anti-LTB4DH (alternative name for PTGR1) antibody (Abnova) at a 1:500 dilution. After washing, the membranes were incubated for 1 h with an anti-mouse peroxidase-conjugated secondary antibody. Chemiluminescence was obtained by adding the Immobilon Western Chemiluminescent HRP Substrate (Millipore), and images were obtained with a digital image VersaDoc™ MP 5000 System (BioRad). The membranes were reprobed with an anti-GSTP1 antibody at a 1:1000 dilution (Sigma Aldrich) followed by a mouse monoclonal anti-actin antibody (Chemicon International).

2.4. Alkenal/one oxidoreductase activity of PTGR1

The NADPH-dependent alkenal/one oxidoreductase activity of PTGR1 was measured according to the continuous spectrophotometric rate determination of NADPH oxidation using trans 2-nonenal as a substrate, according to the method described by Dick et al. (2001). The final reaction consisted of a solution of 0.1 mM trans 2-nonenal, 0.1 mM of NADPH, and 0.2 mg/ml of the protein extract in 50 mM potassium/sodium phosphate buffer, pH 7.0 at 30 °C. The liver protein extracts were obtained in RIPA buffer with a proteinase-inhibitor cocktail as described previously. The oxidation rate of NADPH at 340 nm was monitored for 10 min in two consecutive conditions: without the substrate *trans*-2-nonenal and after the addition of the substrate for another 10 min. The difference in absorbance by minute was obtained, and the enzymatic activity was calculated from the molar extinction coefficient for NADPH (6.2 $(mM\,cm)^{-1}$) and expressed as nmol of NADPH/min/mg of protein.

2.5. Quantitative RT-PCR analysis

Total RNA was obtained from 30 mg of tissue by column-based extraction (RNeasy Mini kit, Qiagen). The cDNA reactions were prepared from 750 ng of total RNA using the High Capacity cDNA Reverse Transcription Kit (Applied Biosystems), and a 1/10 dilution was used for quantitative PCR. The reactions were carried out using TaqMan gene expression assays in an 7900 HT Fast Real Time PCR system (Applied Biosystem, Mexico). FAM dye-labeled probes (exon–exon boundary) for rat *Gstp1* (Rn00561378_gH), *Ptgr1* (Rn00593950_m1), and 18S rRNA (Rn03928990) transcripts were obtained from Applied Biosystems. The *Gstp1* and *Ptgr1* data were normalized against the 18S rRNA gene expression using the comparative Ct method.

2.6. Clinical samples

Paraffin-embedded hepatic biopsies and resection samples from 12 cases of HCC (six females, six males: mean age 54.4 years, range 17–70 years) were obtained from the archive (years: 1993–2008) at the Centro de Especialidades Médicas del Estado de Veracruz, CEMEV, Mexico. The Scientific and Ethical Hospital Committee of CEMEV approved this study (permission number: 005/2011). All

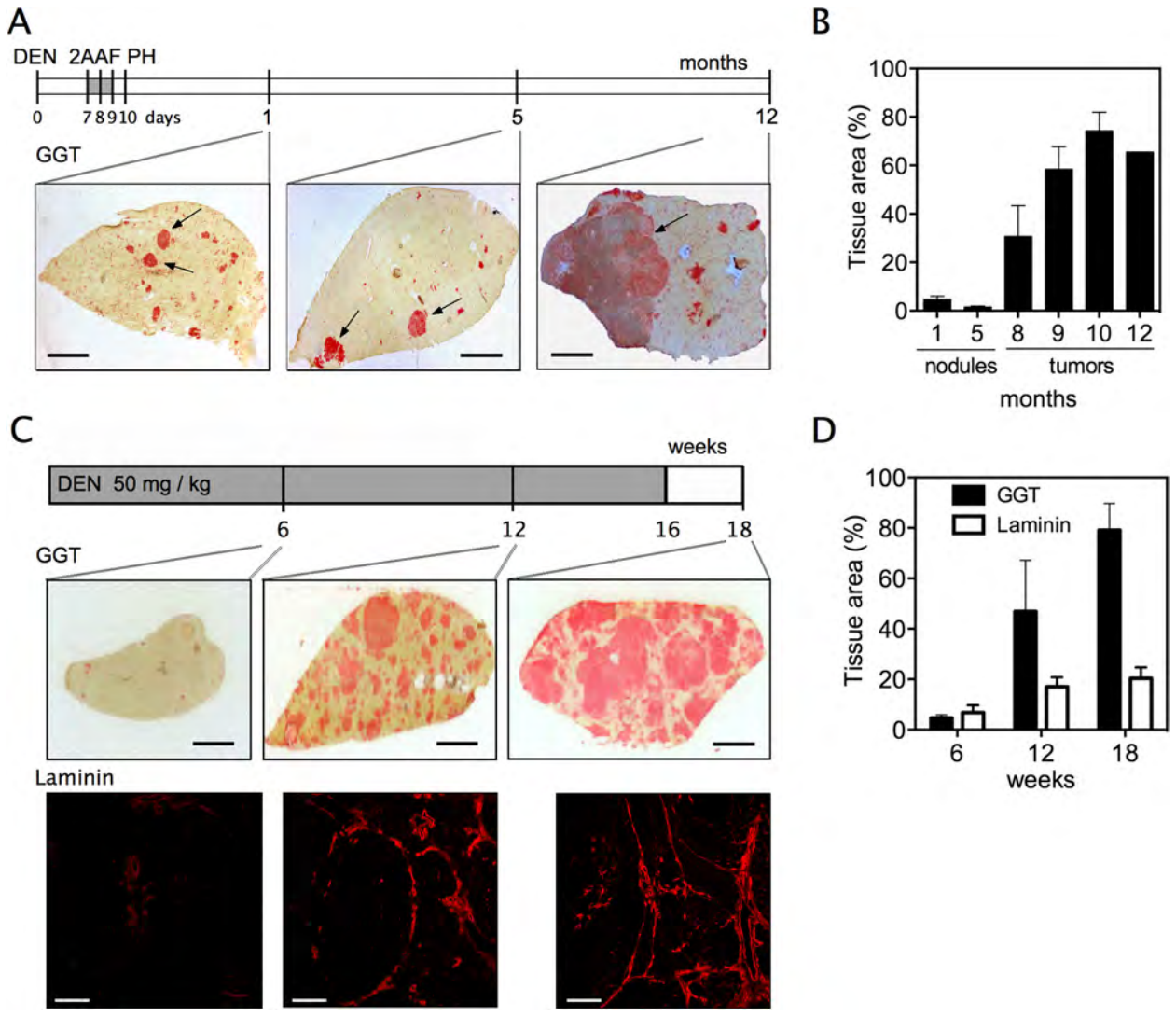

Fig. 1. Two models of chemical hepatocarcinogenesis in rats. (A) The aS&F model (10-day protocol) includes treatments with diethylnitrosamine (DEN), 2-acetylaminofluorene (2AAF) and a 70% partial hepatectomy (PH). Histological sections of livers with GGT⁺ nodules and tumors (arrows) are indicated. (B) Quantitative analysis of GGT⁺ lesions in the liver; this model enabled assessment of the sequential progression of hepatocyte nodules at 1 month to HCCs at 12 months. (C) The Schiffer cirrhosis/cancer protocol consisted of repeated injections of DEN for 16 weeks. Histological sections of livers with GGT⁺ lesions (middle) and liver fibrosis, according to immunofluorescence against laminin (bottom). (D) Quantitative analysis of tissues demonstrating GGT⁺ activity or laminin staining; this model was characterized by cancer progression associated with liver fibrogenesis. Black scale bar correspond to 3 mm. White scale bar correspond to 50 μm.

specimens were sliced and stained with hematoxylin-eosin for routine histological diagnosis. All slides were blindly reviewed by two expert pathologists and confirmed the diagnosis of liver cancer. HCC specimens were grouped as follows according to the tumor grading and the degree of cellular differentiation: well-differentiated ($n = 2$), moderately differentiated ($n = 6$), and poorly differentiated ($n = 4$) (Marcela et al., 2011).

2.7. Immunohistochemistry

Five-micron-thick serial sections were cut from paraffin-embedded hepatic biopsies. The sections of biopsies were deparaffinized, rehydrated, fixed and blocked with 1% BSA for 2 h and then incubated overnight with the primary antibody: either a mouse LT4DH polyclonal antibody (Abnova) at a 1:50 dilution or a mouse glypican-3 (1G12) monoclonal antibody (Cell Marque) at a 1:100 dilution. The rat specimens were incubated with a rabbit PGR1 polyclonal antibody (Novus Biologicals) at a 1:25 dilution and a rabbit polyclonal anti-GSTP antibody (Dako) at a 1:100 dilution. The primary antibodies were detected using the refined avidin–biotin technique with the LSAB + HRP Kit (Dako Corporation, California USA). No staining was observed when the primary antibody was substituted with the mouse or rabbit isotype control.

2.8. Statistical analyses

Statistically significant differences between groups were determined by one-way analysis of variance (ANOVA). Significance was defined as a p-value <0.05.

3. Results

3.1. Comparison of the rat hepatocarcinogenesis models

The aS&F model induced several hepatocyte nodules that were positive for the GGT hepatocarcinogenesis marker and reached diameters of up to 1 mm (Fig. 1A, 1 month), these nodules constituted 4.8% of the liver (Fig. 1B). The hepatocellular tumors reached diameters over 5 mm at 7 to 9 months, exhibited anaplasia under

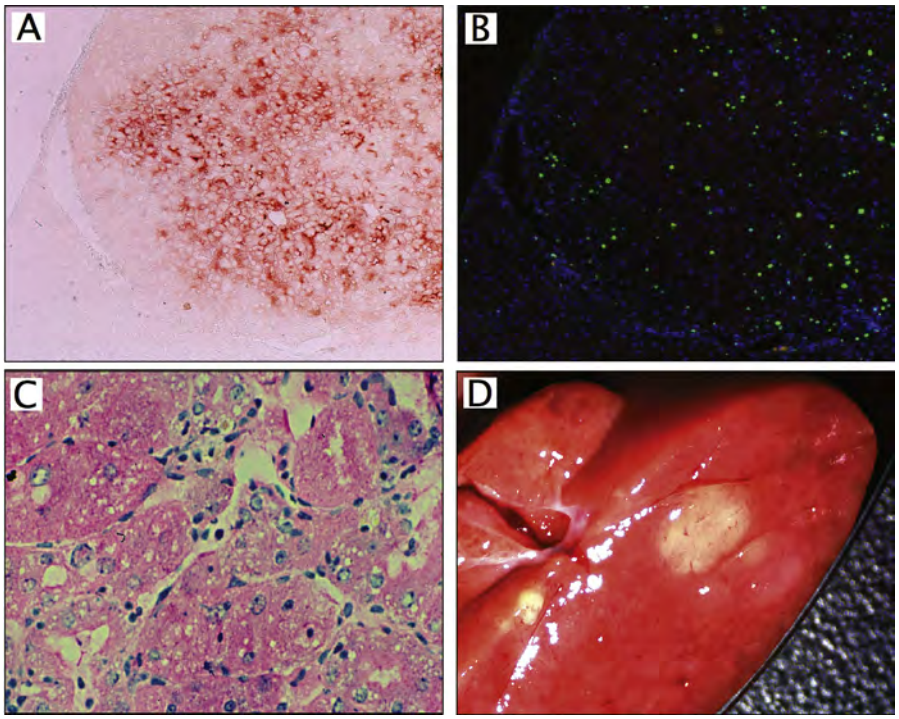

Fig. 2. Representative histological features of nodules and tumors from animals subjected to the aS&F model. A nodule obtained after 5 months displayed (A) GGT activity (red color) and (B) an increased presence of Ki-67-positive cells (green fluorescence) within the nodule; all cellular nuclei were stained with DAPI (blue fluorescence). A tumor obtained after 8 months was (C) stained with H&E and displayed anaplasia, including marked pleomorphism, anisonucleosis, prominent nucleoli, and trabecular enlargement of 3 to 5 cells; upon gross examination, (D) this tumor could be clearly distinguished due to its discolored appearance in comparison to the surrounding tissue. (For interpretation of the references to color in this figure legend, the reader is referred to the web version of this article.)

H&E staining, increased proliferation, discolored appearance and were positive for GGT, as detected by histochemistry (Fig. 2).

The Schiffer protocol induced multiple nodular lesions that were GGT-positive (Fig. 1C). There was also a time-dependent increase in the incidence of these lesions; at week 6, a few small nodules (<0.5 mm diameter) were detected without the presence of fibrotic septa; at week 12, several nodules (<1 mm diameter) were identified and were delimited by fibrotic septa that were laminin-positive; and at week 18, there was an increased proportion of GGT-positive tissue with neoplastic lesions that accumulatively represented up to 80% of the liver (Fig. 1D). The presence of fibrosis was histologically visualized by H&E staining and the laminin fibers by immunofluorescence (Fig. 1C bottom).

3.2. Identification of PTGR1 protein by mass spectrometry

Both tumoral (T) and non-tumoral (NT) tissues were dissected from the frozen livers of rats that had been subjected to the aS&F model, and these tissues were processed to obtain the cytosolic protein fraction. The protein profiles, separated by SDS-PAGE, were very similar between the normal liver (NL) and NT samples, whereas the profiles of the T samples revealed different bands (Fig. 3). In particular, there was an increase in the proteins from 33 to 34 kDa in the T samples. The 33 and 34 kDa protein bands from both the T and NT samples were excised from the polyacrylamide gels and subjected to protein detection by mass spectrometry. Five tumors from four rats were analyzed, and an average of five proteins was identified in each band. It is noteworthy that PTGR1 was the highest-ranked protein repeatedly identified in the tumor bands analyzed and demonstrated the maximum number of peptides matching the protein, with a confidence level >99% (Table 1).

3.3. Increased PTGR1 protein expression and increased alkenal/one oxidoreductase activity

To confirm the presence of PTGR1 in liver neoplasms, Western blot experiments were carried out using the liver samples. Fig. 4A shows the expression of PTGR1, GSTP1, and β-actin from the aS&F

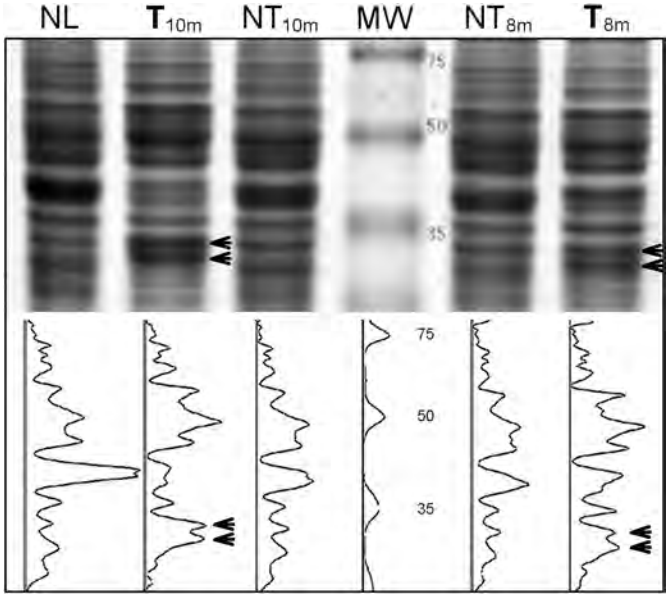

Fig. 3. Differential protein expression analysis of rat liver tumors. Representative electrophoresis gel denoting the protein profiles of hepatic samples, including normal liver (NL), tumor (T) and non-tumor (NT) samples at 8 or 10 months after the initiation of the hepatocarcinogenesis protocol, as indicated. Two different bands at 33 and 34 kDa (arrowheads) were analyzed by mass spectrometry.

Table 1
Identification of PTGR1 protein in liver tumors by MS/MS spectra.

Sample	Type of sample	Statistics of PTGR1 detection				
		Rank[a]	Peptides	Peptides[b] (>99%)	Total ProtScore[c]	% Coverage[d]
T10a-R1	Tumor	1	17	7	14.71	38.30
T10b-R1	Tumor	1	23	9	18.96	63.83
Nt10-R1	Non-tumor	Not found				
T10-R2	Tumor	1	18	7	14.77	38.30
Nt10-R2	Non-tumor	Not found				
T8-R1	Tumor	1	12	3	10.01	31.31
Nt8-R1	Non-tumor	Not found				
T8-R2	Tumor	1	18	4	12.71	34.04
Nt8-R2	Non-tumor	Not found				

[a] The rank of the specified protein relative to all other proteins in the list of detected proteins.
[b] The number of distinct peptides with at least 99% confidence.
[c] A measure of the total amount of evidence for a detected protein, calculated using all of the peptides detected for the protein. For example, each peptide with a confidence >99% contributes 2.0 to the ProtScore.
[d] The percentage of matching amino acids from identified peptides having a confidence value greater than 0 divided by the total number of amino acids in the sequence.

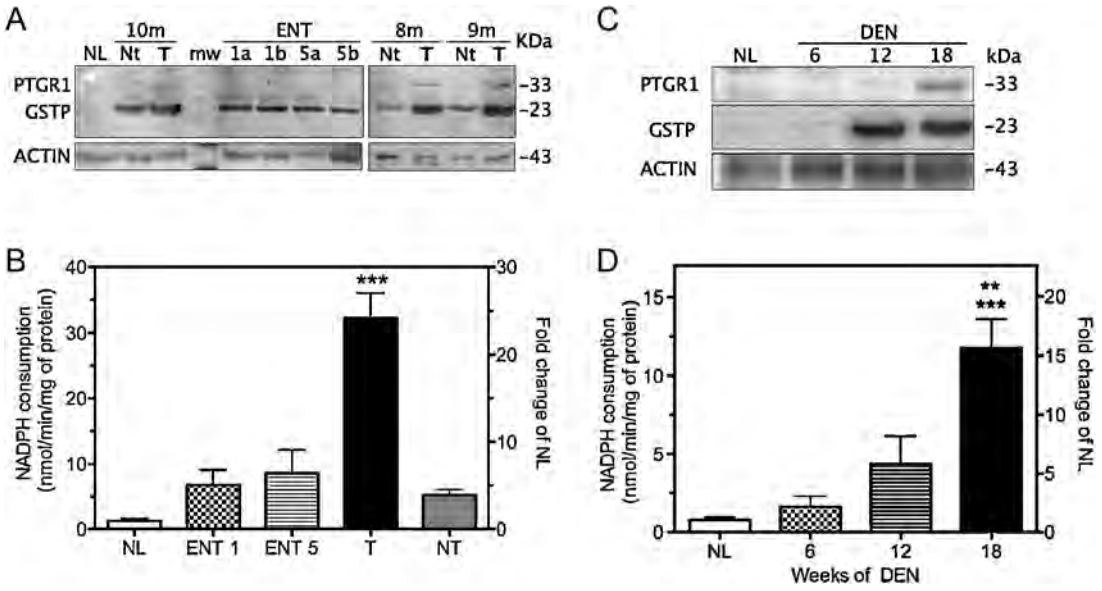

Fig. 4. Increased expression of PTGR1 in hepatocarcinogenesis. Liver samples from the aS&F model. (A) Western blotting using anti-PTGR1, anti-GSTP, and anti-actin antibodies in normal liver (NL), paired non-tumor (NT) and tumor (T) samples at 8, 9 and 10 months and enriched nodular tissue (ENT) samples at 1 and 5 months following protocol initiation. (B) Alkenal/one activity of PTGR1 in the liver extracts. Mean ± SEM; NL, $n = 5$; ENT 1, $n = 3$; ENT 5, $n = 3$; T, $n = 6$; NT, $n = 5$. *** $p < 0.001$ Compared to the other four groups. Liver samples from the Schiffer's model. (C) Western blots in NL and samples from rats sacrificed at 6, 12, and 18 weeks. (D) Alkenal/one activity of PTGR1 in the liver extracts. Mean ± SEM of $n = 5$ for each group. ** $p < 0.01$ Compared to 12 weeks, *** $p < 0.001$ Compared to NL or 6 weeks.

samples; PTGR1 protein was identified as a band of 33 kDa exclusively in the tumor (T) samples at 8, 9, and 10 months. This protein was not identified in non-tumor (NT) tissue, enriched-nodular tissue (ENT), or normal liver (NL) tissue. In the same blot membrane, the hepatocarcinogenesis marker GSTP1 was immunodetected in all samples from rats subjected to the hepatocarcinogenesis protocol. As expected, the NL samples were negative for this protein. Thus, PTGR1 was the only protein detected in this model that was unique to the T samples.

The NADPH alkenal/one oxidoreductase enzymatic activity of PTGR1 in the liver samples is shown in Fig. 4B. The cytosolic extracts of the ENT and NT tissues demonstrated higher activity than the NL tissues. Remarkably, the T samples showed 25-fold greater activity in comparison to NL tissues and 6-fold greater activity in comparison to NT tissues. This elevated enzymatic activity was consistent with the presence of PTGR1 detected in T samples by Western blot.

The extent of PTGR1 protein expression and enzymatic activity were also evaluated in the hepatic tissues of rats sacrificed at 6, 12, and 18 weeks after the induction of Shiffer's model. PTGR1 was only identified in the livers of rats sacrificed at 18 weeks, when the livers contained tumors (Fig. 4C), while GSTP1 was identified in the livers of rats sacrificed from 12 to 18 weeks. The alkenal/one activity of PTGR1 showed a time-dependent increase from 6 to 18 weeks, with the highest enzymatic activity (15-fold higher than NL tissues) at 18 weeks (Fig. 4D).

3.4. Increased gene expression of *Ptgr1*

The gene expression levels of *Ptgr1* and *Gstp1* were obtained by qRT-PCR (Fig. 5). The highest expression of *Ptgr1* was also found in the T samples, with values that ranged from 12- to 200-fold greater when compared to the NT and NL samples from animals subjected to the aS&F model, respectively (Fig. 5A). *Gstp1* was also highly expressed in samples from carcinogen-treated rats, mainly in the T samples, but with a smaller difference in comparison to the ENT and NT tissues (Fig. 5B). In the tumors from Shiffer's model, the expression level of *Ptgr1* was high in the livers of rats sacrificed after 12 to 18 weeks, ranging from 17- to 19-fold higher in comparison to the NL tissues (Fig. 5C). The expression level of *Gstp1* in this model showed a similar profile (Fig. 5D), as it was elevated at 12 and 18

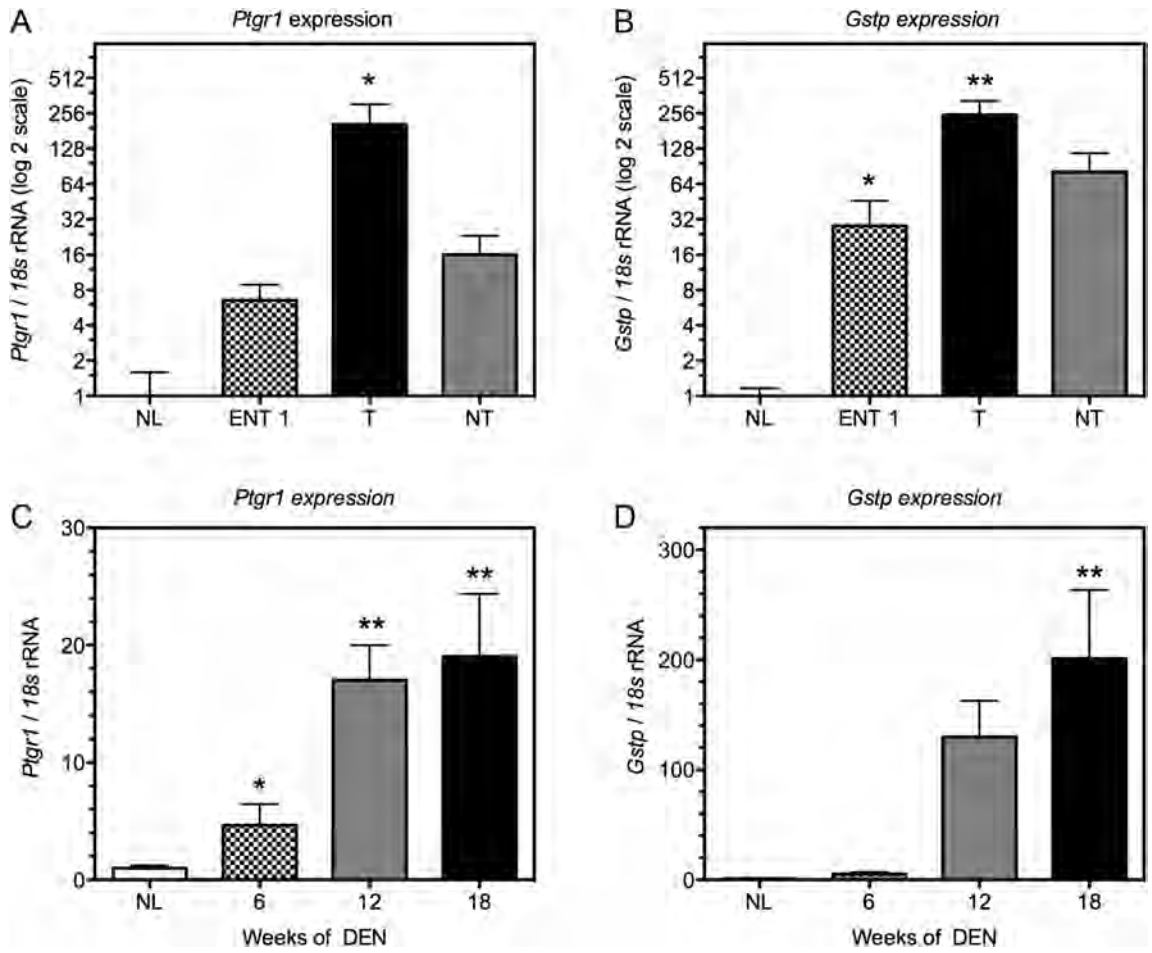

Fig. 5. Increased expression of *Ptgr1* in hepatocarcinogenesis. (A) and (B) qRT-PCR results for *Ptgr1* and *Gstp1* expression in liver lesions induced with the aS&F model. Normal liver (NL), paired non-tumor (NT) and tumor (T), and enriched nodular tissue (ENT) samples obtained 1 month after protocol initiation. (C) and (D) qRT-PCR results for *Ptgr1* and *Gstp1* expression in liver lesions induced with Schiffer's model. NL samples and liver samples from rats treated with DEN that were sacrificed at 6, 12, and 18 weeks. Mean ± SEM of $n = 5$ for each group. For (A) * $p < 0.05$ compared to NL or ENT 1. For (B) ** $p < 0.01$ compared to NL, * $p < 0.05$ compared to T. For (C) ** $p < 0.01$ compared to NL, * $p < 0.05$ compared to 18 weeks. For (D) ** $p < 0.01$ compared to NL or 6 weeks.

weeks but demonstrated a higher fold change in comparison to the expression level of *Ptgr1*.

3.5. Immunohistological expression of PTGR1 in liver tumors

The presence and localization of PTGR1 was analyzed by immunohistochemistry in liver tumor samples obtained from the rat models and human biopsies. High cytoplasmic and nuclear expression was detected in the neoplastic cells of tumors from the aS&F model, while the surrounding NT tissue demonstrated negative expression (Fig. 6A). In a serial section of the same specimen, GSTP1 expression was detected in the cytoplasm of tumor cells. Moreover, PTGR1 was expressed in 12 human HCC biopsies (Fig. 6B). When the HCC specimens were classified according to their degree of differentiation, two were well-differentiated, six were moderately differentiated, and four were poorly differentiated. All HCC samples were stained with moderate intensity in comparison to non-cancerous liver, the parenchymal tissue of a patient with fibrosis. To verify the neoplastic nature of HCC, immunohistochemistry specific for glypican-3 was performed in serial sections of the same specimens (Fig. 6B). This protein is a known marker for HCC and is not expressed in benign hepatic disorders (Zhu et al., 2001).

4. Discussion

In this study, we induced two models of rat hepatocarcinogenesis: the aS&F model and Schiffer's model. When proteins derived from these rat tumors were analyzed by SDS-PAGE, different protein bands were found in comparison to those from NT tissue, and mass spectrometry analysis of these bands led to the identification of PTGR1. The high expression of this enzyme in experimental tumors was confirmed by Western blotting analysis, immunohistochemistry, and the observed increase in alkenal/one oxidoreductase activity. Concordant with these data, increased gene expression of *Ptgr1* was identified by qRT-PCR. Furthermore, PTGR1 expression was increased in the cytoplasm of neoplastic cells from human HCC specimens. Thus, the increased expression of PTGR1 in both the experimental tumors of rats and the human biopsy samples may reflect molecular similarities between hepatocarcinogenesis in rats and humans that are independent of the pathological context of cirrhosis.

PTGR1 has been given alternative names depending on the molecular function identified for this enzyme, including NADP-dependent leukotriene B4, 12-hydroxydehydrogenase, 15-oxoprostaglandin 13-reductase, NADPH-dependent alkenal/one oxidoreductase, zinc-binding alcohol dehydrogenase domain-containing protein 3, and dithiolethione-inducible gene 1 (DIG-1).

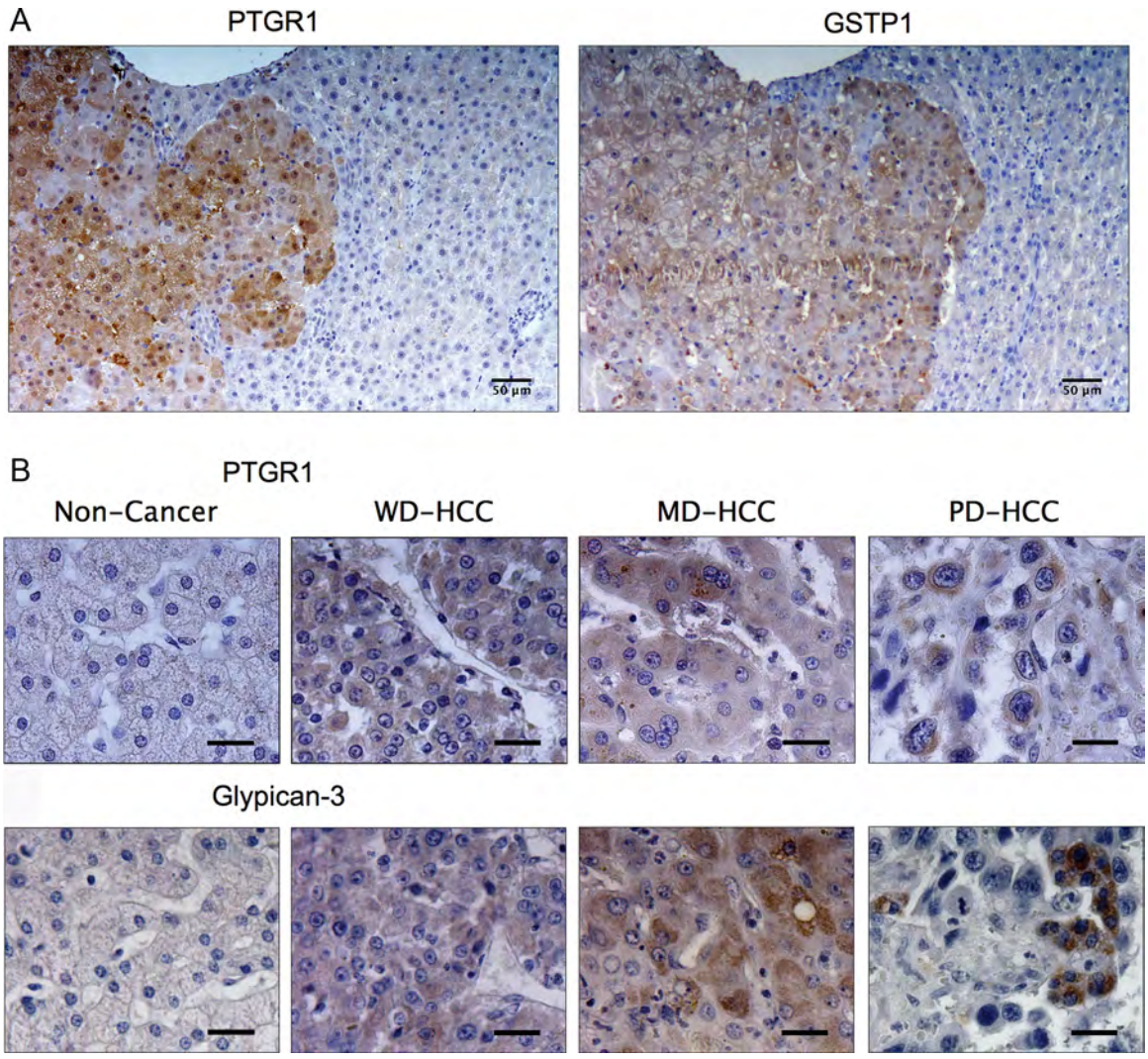

Fig. 6. PTGR1 expression in liver tumors by immunohistochemistry. (A) Presence of PTGR1 and GSTP1 in serial sections of a 9-month tumor obtained from the αS&F model. (B) PTGR1 and glypican-3 expression in human HCC tissues. Representative images of a non-cancerous liver and well-differentiated (WD), moderately differentiated (MD), and poorly differentiated (PD) HCC tissues. Magnification in (A) 200×, scale bar 50 μm; (B) 400×; scale bar 25 μm.

PTGR1 is a key enzyme responsible for the biological catabolism of prostaglandins and some eicosanoids (Tai et al., 2002). In addition, this enzyme reduces α,β unsaturated carbonyls, which are often produced in the cell under oxidative stress as lipid peroxidation by-products such as 4-hydroxy-2-nonenal (4HNE). 4HNE and other aldehydes derive from the peroxidation of linoleic and arachidonic acid (Spitz et al., 1990) and have important cytotoxic effects on cells, ranging from the inhibition of both DNA and protein synthesis to the induction of cell death (Chaudhary et al., 2010; Forman et al., 2008). Furthermore, the alkenal/one oxidoreductase activity of PTGR1 has demonstrated the capacity to metabolize 4HNE into 4-hydroxy nonanal (4HNA) through reduction of the α,β-double bond (Dick et al. 2001; Youn et al., 2006), and it has therefore been proposed to function as a cytoprotective enzyme. In fact, cells transfected with an episomal vector overexpressing *Ptgr1* showed increased cell viability under the presence of 4HNE and a reduced level of 4HNE protein adducts when compared to cells without PTGR1 activity (Dick et al. 2001). PTGR1 was also described as a gene that could be induced by dithiolethiones (Primiano et al., 1996, 1998), a well-known class of cancer chemopreventive agents that induce carcinogen-detoxification enzymes such as NAD(P)H dehydrogenase, quinone 1 (NQO1), several glutathione *S*-transferases (GSTs), epoxide hydrolase (EPHX), glutamate-cysteine ligase (GCL), and UDP glucuronosyltransferases (UGTs) through activation of the Keap1-Nrf2 pathway (Zhang and Munday, 2008). All of these observations support the notion that PTGR1 acts as a cytoprotective enzyme that has both antioxidative and anti-inflammatory functions.

Since there are no previous reports showing altered expression of PTGR1 in tumors, the role of this enzyme in tumorigenesis remains to be elucidated. The PTGR1 has antioxidative and antiinflamatory enzymatic properties that may allow its consideration as a tumor suppressor. In agreement with this, the restored expression of PTGR1 by recombinant adenovirus infection in the lung cancer cell lines with negative or low PTGR1 expression (H1299 and A549, respectively) induces apoptosis, cell growth suppression and reduced tumorigenesis when transfected cells are injected to nude mice (Zhao et al., 2010). Contrastingly this study also showed that the lung cancer cell line (H157) with high constitutive PTGR1 expression was unaffected in apoptosis and growth inhibition. *Ptgr1* expression seems to be regulated by the transcription factor Nrf2, this factor, when is constitutively active by oncogenes, mutations or other mechanism, may stimulate a cellular antioxidant program that promotes detoxification of oxidative by products and also induces tumorigenesis (DeNicola et al., 2011). Other important aspect to understand the role of PTGR1 in tumors is the imbalance

of its substrates/products that can promote tumor growth. Most of the PTGR1-substrates; prostaglandins, leukotrienes and lipid peroxidation products such as 4-HNE have multifaceted inflammatory and redox roles that may promote an altered cell signaling that contributes to HCC development (Chaudhary et al., 2010; Kundu and Surh, 2012). Although we believe that the increased PTGR1 expression in tumors may confer metabolic resistance to the toxicity of endogenous lipid peroxidation products, further studies should be carried out to elucidate the functional role of this enzyme in neoplastic liver cells.

Although the elucidation of a possible mechanism of action of PTGR1 during tumorigenesis may provide data to point this enzyme as a possible therapeutic target for liver cancer, it is remarkable that tumors with an increased PTGR1 expression acquire metabolic properties that can be used for pharmacological experimentation. Indeed, rat liver tumors showed an increased capacity to reduce the α,β unsaturated aldehyde (trans 2-nonenal) 25-fold more than the normal liver (Fig. 4B). This alkenal/ona oxidoreductase property of tumors could be used for activation of antitumoral drugs such as the acylfulvene. This selective antitumor drug and its analogous are activated by PTGR1 for their DNA-alkylating activity (Erzinger and Sturla, 2011; Gong et al., 2007; Pietsch et al., 2011; Yu et al., 2012). *Ptgr1* is an inducible gene with minimal or absent expression in normal liver cells but is overexpressed in tumor cells, which may makes it conducive to the assessment of tumor pharmacological therapy. Furthermore, our group is currently exploring the idea that PTGR1, through its alkenal/one oxidoreductase activity, may be important for the bioactivation of certain substances into cytotoxic metabolites in tumor cells. In this manner, cancer cells expressing PTGR1 may be more susceptible than normal cells to cytotoxic agents that are activated by bioreduction. Determination of increased PTGR1 expression in HCC patients would be an important biomarker to select those candidates for antitumoral therapy, specifically with drugs that become cytotoxic by activity of this enzyme.

In experimental models, carcinogen-initiated hepatocytes form foci and nodules of altered hepatocytes, some of which evolve into malignant tumors through a cellular selection process (Farber and Sarma, 1987). The increased expression of enzymatic markers such as GSTP1 and GGT can be observed in these lesions, even during the early stages in initiated hepatocytes and altered foci (Sato, 1989; Yusof et al., 2003). The increased expression of PTGR1, as described here, is more commonly associated with the progression stage of hepatocarcinogenesis than with the earlier stages of initiation and promotion. PTGR1 was detected in tumor samples only after 8 months in the aS&F model; similarly, in Schiffer's model, PTGR1 was detected in livers that contained tumors at 18 weeks. Furthermore, the enzymatic activity of PTGR1 was increased in both tumors and liver tissue at 18 weeks, supporting the idea that PTGR1 overexpression is a specific molecular change of neoplastic cells that may serve as a marker for advanced nodules and tumors.

We detected the presence of PTGR1 in a dozen human HCCs that were also glypican-3-positive by immunohistochemistry. In particular, PTGR1 protein was localized to the cytoplasm of neoplastic cells in all samples examined; although PTGR1 expression did not correlate with the degree of differentiation, its expression was heterogeneous in poorly differentiated cancer samples, similar to glypican-3 expression. Additional data related to the protein expression of PTGR1 in human liver tumors is publicly available on the Human Protein Atlas portal (http://www.proteinatlas.org), which is a resource for immunohistochemistry-based maps of protein expression (more than 12,200 proteins) that is useful for pathological research (Ponten et al., 2008). Among the 23 cases with liver cancer in this portal, 19 were PTGR1-positive. The majority (11/15) were HCCs with >75% positive cells , while only 1/8 cholangiocarcinomas showed >75% positive cells (Supplementary Fig. S1). Gene expression data of human HCC also revealed increased expression of *Ptgr1* (Ho et al., 2012; Hoshida et al., 2009). *Ptgr1* is shown in the list of up-regulated genes obtained by RNA-sequencing in CD90$^+$ cancer stem cells compared to CD90$^+$ non-tumor stem cell obtained from three HCC patients (Ho et al., 2012). A meta-analysis of gene expression profiles in data sets from eight independent patient cohorts (603 patients) revealed three subclasses of HCC (termed S1–S3) (Hoshida et al., 2009). The hierarchical clustering of this study contained *Ptgr1* (named LTB4DH) in the gene signature for S3 HCC. The subclass 3 included the majority of well- and moderate- differentiated HCCs and it was associated with a hepatocyte-like phenotype. It seems that PTGR1 is more highly expressed in HCCs than in cholangiocarcinomas, specifically associated to a subclass 3 of HCC according to genomic classification and expressed in cancer stem cell CD90$^+$. Considering these data, our study allows us to propose that the increased expression of Ptgr1 may have a clinical value for HCC. However, further studies with different types of liver cancers, different etiologies, and histological grading from dysplasia to advanced neoplasia should be performed to determine whether the PTGR1 expression level might be used as a biomarker for diagnosis and prognosis purposes.

Our results showing increased PTGR1 expression and activity in experimental hepatocarcinogenesis models and clinical liver tumors encourage research aimed at understanding the metabolic role of PTGR1 in liver tumorigenesis. Furthermore, our findings contribute to understanding the biochemical features of HCCs and may be used to design new therapies for HCC.

Acknowledgments

We greatly appreciate technical assistance of Karol Carrillo, Valeria Quintanar, Fabiola Morales and Raul Mojica from our institutional high technology units. R.S.R. is supported by a fellowship from CONACYT 421197, and this study is part of his doctoral thesis from the Biomedical Sciences Doctorate Program, Faculty of Medicine, Universidad Nacional Autónoma de México. This work was supported by the Fondo Sectorial de Investigación en Salud y Seguridad Social SSA/IMSS/ISSSTE-CONACYT SALUD-2009-01-115431.

Appendix A. Supplementary data

Supplementary data associated with this article can be found, in the online version, at http://dx.doi.org/10.1016/j.biocel.2014.05.017.

References

Carrasco-Legleu CE, Marquez-Rosado L, Fattel-Fazenda S, Arce-Popoca E, Perez-Carreon JI, Villa-Trevino S. Chemoprotective effect of caffeic acid phenethyl ester on promotion in a medium-term rat hepatocarcinogenesis assay. Int J Cancer 2004;108:488–92.

Clish CB, Levy BD, Chiang N, Tai HH, Serhan CN. Oxidoreductases in lipoxin A4 metabolic inactivation: a novel role for 15-onoprostaglandin 13-reductase/leukotriene B4 12-hydroxydehydrogenase in inflammation. J Biol Chem 2000;275:25372–80.

Chaudhary P, Sharma R, Sharma A, Vatsyayan R, Yadav S, Singhal SS, et al. Mechanisms of 4-hydroxy-2-nonenal induced pro- and anti-apoptotic signaling. Biochemistry 2010;49:6263–75.

DeNicola GM, Karreth FA, Humpton TJ, Gopinathan A, Wei C, Frese K, et al. Oncogene-induced Nrf2 transcription promotes ROS detoxification and tumorigenesis. Nature 2011;475:106–9.

Dick RA, Kensler TW. The catalytic and kinetic mechanisms of NADPH-dependent alkenal/one oxidoreductase. J Biol Chem 2004;279:17269–77.

Dick RA, Kwak MK, Sutter TR, Kensler TW. Antioxidative function and substrate specificity of NAD(P)H-dependent alkenal/one oxidoreductase. A new role for leukotriene B4 12-hydroxydehydrogenase/15-oxoprostaglandin 13-reductase. J Biol Chem 2001;276:40803–10.

El-Serag HB, Marrero JA, Rudolph L, Reddy KR. Diagnosis and treatment of hepatocellular carcinoma. Gastroenterology 2008;134:1752–63.

Erzinger MM, Sturla SJ. Bioreduction-mediated food-drug interactions: opportunities for oncology nutrition. Chimia (Aarau) 2011;65:411–5.
Farber E, Sarma DS. Hepatocarcinogenesis: a dynamic cellular perspective. Lab Invest 1987;56:4–22.
Forman HJ, Fukuto JM, Miller T, Zhang H, Rinna A, Levy S. The chemistry of cell signaling by reactive oxygen and nitrogen species and 4-hydroxynonenal. Arch Biochem Biophys 2008;477:183–95.
Gong J, Vaidyanathan VG, Yu X, Kensler TW, Peterson LA, Sturla SJ. Depurinating acylfulvene-DNA adducts: characterizing cellular chemical reactions of a selective antitumor agent. J Am Chem Soc 2007;129:2101–11.
Ho DW, Yang ZF, Yi K, Lam CT, Ng MN, Yu WC, et al. Gene expression profiling of liver cancer stem cells by RNA-sequencing. PLoS One 2012;7:e37159.
Hori T, Yokomizo T, Ago H, Sugahara M, Ueno G, Yamamoto M, et al. Structural basis of leukotriene B4 12-hydroxydehydrogenase/15-Oxo-prostaglandin 13-reductase catalytic mechanism and a possible Src homology 3 domain binding loop. J Biol Chem 2004;279:22615–23.
Hoshida Y, Nijman SM, Kobayashi M, Chan JA, Brunet JP, Chiang DY, et al. Integrative transcriptome analysis reveals common molecular subclasses of human hepatocellular carcinoma. Cancer Res 2009;69:7385–92.
Kundu JK, Surh YJ. Emerging avenues linking inflammation and cancer. Free Radic Biol Med 2012;52:2013–37.
Libbrecht L, Desmet V, Roskams T. Preneoplastic lesions in human hepatocarcinogenesis. Liver Int 2005;25:16–27.
Marcela S, Elizabeth M, Jay HL. Recent advances in the classification of hepatocellular carcinoma. Diagn Histopathol (Oxf) 2011;18:37–45.
Marche-Cova A, Fattel-Fazenda S, Rojas-Ochoa A, Arce-Popoca E, Villa-Trevino S. Follow-up of GST-P during hepatocarcinogenesis with DEN-2AAF in F344 rats. Arch Med Res 1995;26(Spec No):S169–73.
Perez-Carreon JI, Lopez-Garcia C, Fattel-Fazenda S, Arce-Popoca E, Aleman-Lazarini L, Hernandez-Garcia S, et al. Gene expression profile related to the progression of preneoplastic nodules toward hepatocellular carcinoma in rats. Neoplasia 2006;8:373–83.
Perez E, Gallegos JL, Cortes L, Calderon KG, Luna JC, Cazares FE, et al. Identification of latexin by a proteomic analysis in rat normal articular cartilage. Proteome Sci 2010;8:27.
Pietsch KE, Neels JF, Yu X, Gong J, Sturla SJ. Chemical and enzymatic reductive activation of acylfulvene to isomeric cytotoxic reactive intermediates. Chem Res Toxicol 2011;24:2044–54.
Ponten F, Jirstrom K, Uhlen M. The human protein Atlas—a tool for pathology. J Pathol 2008;216:387–93.
Primiano T, Gastel JA, Kensler TW, Sutter TR. Isolation of cDNAs representing dithiolethione-responsive genes. Carcinogenesis 1996;17:2297–303.
Primiano T, Li Y, Kensler TW, Trush MA, Sutter TR. Identification of dithiolethione-inducible gene-1 as a leukotriene B4 12-hydroxydehydrogenase: implications for chemoprevention. Carcinogenesis 1998;19:999–1005.
Sato K. Glutathione transferases as markers of preneoplasia and neoplasia. Adv Cancer Res 1989;52:205–55.
Schiffer E, Housset C, Cacheux W, Wendum D, Desbois-Mouthon C, Rey C, et al. Gefitinib, an EGFR inhibitor, prevents hepatocellular carcinoma development in the rat liver with cirrhosis. Hepatology 2005;41:307–14.
Solt D, Farber E. New principle for the analysis of chemical carcinogenesis. Nature 1976;263:701–3.
Spitz DR, Malcolm RR, Roberts RJ. Cytotoxicity and metabolism of 4-hydroxy-2-nonenal and 2-nonenal in H_2O_2-resistant cell lines. Do aldehydic by-products of lipid peroxidation contribute to oxidative stress? Biochem J 1990;267:453–9.
Tai HH, Ensor CM, Tong M, Zhou H, Yan F. Prostaglandin catabolizing enzymes. Prostaglandins Other Lipid Mediat 2002;68–69:483–93.
Vitturi DA, Chen CS, Woodcock SR, Salvatore SR, Bonacci G, Koenitzer JR, et al. Modulation of nitro-fatty acid signaling: prostaglandin reductase-1 is a nitroalkene reductase. J Biol Chem 2013;288:25626–37.
Wu L, Tang ZY, Li Y. Experimental models of hepatocellular carcinoma: developments and evolution. J Cancer Res Clin Oncol 2009;135:969–81.
Youn B, Kim SJ, Moinuddin SG, Lee C, Bedgar DL, Harper AR, et al. Mechanistic and structural studies of apoform, binary, and ternary complexes of the Arabidopsis alkenal double bond reductase At5g16970. J Biol Chem 2006;281:40076–88.
Yu X, Egner PA, Wakabayashi J, Wakabayashi N, Yamamoto M, Kensler TW. Nrf2-mediated induction of cytoprotective enzymes by 15-deoxy-Delta12,14-prostaglandin J2 is attenuated by alkenal/one oxidoreductase. J Biol Chem 2006;281:26245–52.
Yu X, Erzinger MM, Pietsch KE, Cervoni-Curet FN, Whang J, Niederhuber J, et al. Up-regulation of human prostaglandin reductase 1 improves the efficacy of hydroxymethylacylfulvene, an antitumor chemotherapeutic agent. J Pharmacol Exp Ther 2012;343:426–33.
Yusof YA, Yan KL, Hussain SN. Immunohistochemical expression of pi class glutathione *S*-transferase and alpha-fetoprotein in hepatocellular carcinoma and chronic liver disease. Anal Quant Cytol Histol 2003;25:332–8.
Zhang Y, Munday R. Dithiolethiones for cancer chemoprevention: where do we stand? Mol Cancer Ther 2008;7:3470–9.
Zhao Y, Weng CC, Tong M, Wei J, Tai HH. Restoration of leukotriene B(4)-12-hydroxydehydrogenase/15-oxo-prostaglandin 13-reductase (LTBDH/PGR) expression inhibits lung cancer growth in vitro and in vivo. Lung Cancer 2010;68:161–9.
Zhu ZW, Friess H, Wang L, Abou-Shady M, Zimmermann A, Lander AD, et al. Enhanced glypican-3 expression differentiates the majority of hepatocellular carcinomas from benign hepatic disorders. Gut 2001;48:558–64.